2013

Efficient Numerical Scheme of the Dynamics of Nonisothermal Thin Film Flow

Moustafa A. Soliman
The British University in Egypt, moustafa.aly@bue.edu.eg

Khalid I. Alhumaizi
King Saud University, humaizi@ksu.edu.sa

Efficient Numerical Scheme of the Dynamics of Nonisothermal Thin Film Flow

Moustafa A. Soliman[a,b] & Khalid Alhumaizi[a]
a- Chemical Engineering Department, College of Engineering
King Saud University
P.O. Box 800, Riyadh 11421, Saudi Arabia
b- Chemical Engineering Department, College of Engineering
The British University in Egypt
El-Sherouk City, Egypt
e-mail:Moustafa.aly@bue.edu.eg

***Abstract*--** **In this work we use Lubrication type method, based on the possibility of the separation of longitudinal and transversal length scales to simplify the analysis of thin film dynamics. We study the dynamics of evaporating thin liquid films on an inclined plane, where the effect of van der Waal forces is significant. The numerical solution of the evolution equation is carried out using the method of orthogonal collocation and is used for the study of the instabilities of evaporating thin film to identify conditions for efficient operation. For symmetric cases where the plane is horizontal, a two spline collocation second order formulation method that makes use of the symmetry seems most appropriate. For inclined plane, a spline collocation first order formulation method is most efficient.**

***Index Term*--** **Thin film flow, lubrication theory , orthogonal collocation**

I. INTRODUCTION

The study of supported thin film on plane and inclined surfaces phenomena has been motivated both by their scientific and industrial applications. Thin films are of great importance in industrial applications such as cooling, lubrication, cleaning, painting, spraying, adhesion, and protective coatings among others. Some of these techniques are linked to the rapidly expanding fields of micro-fluidics and nanotechnologies. In some of these thin film applications, it is desirable to maintain a smooth film surface, and it is therefore crucial that the film remains stable over time. However, it is known that liquid films can start to flow, e.g. under the influence of intermolecular forces, with the result that the uniform film sometimes ruptures into a pattern of droplets or holes.

The primary factors affecting the interfacial dynamics of thick films are: mean flow (destabilizing), surface tension (stabilizing), and thermocapillary (destabilizing). While for thin films, long range intermolecular forces owing to van der Waals interactions significantly affect the stability of the film, these do not affect the thick films.

The mathematical modeling of the hydrodynamics of thin film leads to a system of equations based on Navier-Stokes, energy and continuity equations. However simplifications are possible. If the ratio of the mean film thickness to the wavelength of the surface waves (epsilon) is small, the system equations can be expanded in terms of epsilon leading to a single partial differential equation giving the dynamics of the liquid film thickness. This approximation is known as long wave approximation or lubrication theory.

Burelbach et al. [1] studied the stability of evaporating films on a horizontal plane. They considered the effect of vapour recoil, , surface tension, thermocapillarity and van der Waals forces. Joo et al. [2] studied the same problem but on an inclined plane where gravitational forces are important. They neglected the effect of van der Waal forces. Ali, et.al., [3] studied the stability and rupture of nano-liquid films flowing down an inclined plate and they accounted for gravity and van der Waals forces.

Miladinova and Lebon [4] studied the same problem as in [2] and introduced the effect of nonuniform heating.

References [1,2] used the finite difference method to solve the governing equations. Momoniat et al [6] developed a Crank-Nicholson implicit-explicit scheme for solving the generalized lubrication equation. Cueto-Felgueroso et al [7] presented a rational spectral method for non-linear fourth order equations. In this paper we solve the governing equations using different schemes based on the collocation method.

II. PROBLEM FORMULATION

We consider a two-dimensional Newtonian liquid of a constant density ρ and viscosity μ, driven by gravity and van der Waals force down an isothermal plane inclined at an angle Θ, as shown in Fig. 1. The plate has a constant temperature T_H and the temperature T_F of the liquid on the free surface is controlled by losses to the passive gas above. The liquid evaporate at the free surface. The thermocapillary effects occur due to the dependence of surface tension on temperature. A two dimensional Cartesian coordinate is used to describe the problem with x directed down the plate and z normal to the plate as shown in Fig. 1. The flow is described by a two-dimensional Navier–Stokes equation coupled with continuity equation and associated boundary conditions. The body force term in the Navier–Stokes equation was modified by the inclusion of excess intermolecular interactions between fluid film and the solid surface owing to long range van der Waals force, in addition to gravity force. The lubrication type approximation is used to describe the system in terms of the following dimensionless dependent variables:

$$\xi = \varepsilon x, \quad \varsigma = z, \quad \tau = \varepsilon t$$

where ε is the small wave number defined as the ratio of the mean thickness of the layer to a characteristics length in the x-direction which typically is proportional to the disturbance wavelength. The evolution equation for the film thickness h is derived [1,2]to be:

$$h_\tau + \frac{\bar{E}}{h+K} + \overbrace{Gh^2 h_\xi \sin\theta}^{\text{Wave propoagatiuon}}$$
$$+\varepsilon\left[\overbrace{\frac{2G^2}{15}h^6 h_\xi \sin^2\theta}^{\text{Mean shear flow}} + \overbrace{\frac{KM}{P}\frac{h^3 h_\xi}{(h+K)^3}}^{\text{Thermocapillarity}} + \overbrace{\frac{E^2}{D}\frac{h^3 h_\xi}{(h+K)^3}}^{\text{Vapor recoil}} - \overbrace{\frac{1}{3}Gh^3 h_\xi \cos\theta}^{\text{hydrostatic}} + \overbrace{\bar{S}h^3 h_{\xi\xi\xi}}^{\text{Surface tension}} + \overbrace{\frac{A}{h}h_\xi}^{\text{van der Wall}}\right]_\xi$$
$$+\varepsilon\bar{E}\frac{5G}{24}\left(\frac{h^4}{h+K}\right)_\xi \sin\theta + \varepsilon\bar{E}P\left(\frac{h}{h+K}\right)^3\left[\frac{\bar{E}}{3(h+K)} + \frac{G}{120}(7h-15K)hh_\xi \sin\theta\right] = 0,$$

(1)

Equation (1) is fourth-order partial differential equation and it contains several parameters which represent the effects of all considered phenomena on the dynamics of the film thickness. The parameter E is the evaporation number and all terms proportional to E describe the mass loss due to evaporation. G is gravity number and it appears on the third term and the seventh term: the third term describes the wave propagation and steepening while the other term represents the hydrostatic effect. The G appears also on the fourth term which represent the mass shear flow due to gravity. The fifth term represents the thermocapilarity effect written in term of the Marangoni number M, K and Prandtel number P. K is a measure number for the degree of non-equilibrium on the free surface (K=0 represents the case of a constant free surface temperature while large K gives the zero-evaporation limit). The vapor recoil effects appears on the sixth term of the evolution equation. The eighth term represents the effect of the surface tension. The last term written in term of the parameter *A* represent the molecular van der Waal forces effect.

The dynamics of thin falling film of a Newtonian liquid on an inclined heated surface is represented by a nonlinear fourth order partial differential equation defined (1) describe the dynamic behavior of a nonisothermal thin film subjected to interfacial surface tension and intermolecular van der Waals forces.

Equation (1) is defined with periodic boundary conditions over a non-dimensional wave length (2π/k):

$$\left(\frac{\partial^i h}{\partial \xi^i}\right)_{\xi=0} = \left(\frac{\partial^i h}{\partial \xi^i}\right)_{\xi=2\pi/k} \qquad i = 0,1,2,3; \qquad 0 \le \xi \le \frac{2\pi}{k}$$

(2)

A periodic initial condition is used

$$h(0,\xi) = 1 + \delta\sin(k\xi) \qquad |\delta| \langle 1|$$

(3)

The only force which increases as the film gets thinner is the van der Waal Force. The linear stability analysis gives us an expression for the growth rate. For stability the growth rate should be negative. When the growth rate is zero, we obtain a cutoff wavenumber which indicates neutral stability. For $0<k<k_c$, we have instability, i.e., small disturbance grows. For maximum growth rate; we get k_m; the maximizing wavenumber ($k_m<k_c$)

$$k_m = k_c / \sqrt{2}$$

(4)

III. NUMERICAL METHOD

Dynamic models for thin liquid falling films require suitable numerical procedures to solve the partial differential equation set that describes the film thickness dynamics. The orthogonal collocation method has been applied for different problems in several chemical engineering applications [8-10]. In this method, a trial function is taken as a series of orthogonal polynomials whose roots are used as collocation points (thus avoiding an arbitrary choice by the user) and the dependent variables become the solution values at these collocation points. The accuracy of the method increases rapidly with the order of the trial function but a first-order approximation usually gives good results. In addition, the method has an additional advantage of reducing by 50% the number of unknown variables if solution of the model is symmetric. In particular, it is shown that for an nth-order differential equation in one space dimension with two-point derivative boundary conditions, an ideal choice of interior collocation points is the set of zeros of a Jacobi polynomial. The Jacobi polynomials $P_n^{(\alpha,\beta)}(x)$ are defined such that they satisfy the orthogonality conditions [9,10]

$$\int_0^1 w(x)P_n^{(\alpha,\beta)}(x)P_m^{(\alpha,\beta)}(x)dx = 0 \qquad (n \ne m)$$

(5)

and

$$\int_0^1 w(x)P_n^{(\alpha,\beta)}(x)P_m^{(\alpha,\beta)}(x)dx = C_n \succ 0 \qquad (n=m)$$

(6) where w(x) is the weighting function for the orthogonality conditions. For Jacobi polynomials,

$$w(x) = (1-x)^{\alpha} x^{\beta} \quad , \quad \alpha,\beta \rangle -1 \tag{7}$$

Thus $P_n^{(\alpha,\beta)}$ (x) is the orthogonal polynomial of degree n and α,β are the indices of the weighting function. C_n is a constant.

In the following we present the formulation of the problem in term of the orthogonal collocation method. Consider

$$\eta = \frac{k\,\xi}{2\pi} \tag{8}$$

Equation (1) can be written in term of this new variable as follows:

$$h_t + \frac{\varepsilon k^2}{4\pi^2}\left[\frac{\bar{S}k^2}{4\pi^2}h^3 h_{\eta\eta\eta} + h_\eta\left[\frac{A}{h} + \frac{2G^2}{15}h^6\sin^2\theta + \frac{KM}{P}\left(\frac{h}{h+K}\right)^2 + \frac{E^2}{D}\left(\frac{h}{h+K}\right)^3 - \frac{1}{3}Gh^3\cos\theta\right]\right]_\eta$$
$$+\frac{\bar{E}}{h+K} + Gh^2\frac{k}{2\pi}h_\eta\sin\theta + \varepsilon\bar{E}\frac{5G}{24}\frac{k}{2\pi}\left(\frac{h^4}{h+K}\right)_\eta\sin\theta +$$
$$\varepsilon\bar{E}\left(\frac{h}{h+K}\right)^3\left[\frac{\bar{E}}{3(h+K)} + \frac{k}{2\pi}\frac{G}{120}(7h-15K)hh_\eta\sin\theta\right] = 0 \tag{9}$$

Which can be written in the following form:

$$h_t + \frac{k^2\varepsilon}{4\pi^2}\left[\begin{array}{l}\frac{k^2\bar{S}}{4\pi^2}\left(h^3 h_{\eta\eta\eta\eta} + 3h^2 h_\eta h_{\eta\eta\eta}\right) + \\ h_{\eta\eta}\left(\frac{A}{h} + \frac{2G^2}{15}h^6\sin^2\theta + \frac{KM}{P}\left(\frac{h}{h+K}\right)^2 + \frac{E^2}{D}\left(\frac{h}{h+K}\right)^3 - \frac{1}{3}Gh^3\cos\theta\right) + \\ h_\eta^2\left[\frac{-A}{h^2} + \frac{2}{3}G^2h^5\sin^2\theta + \frac{2K^2Mh}{(h+K)^3P} + \frac{3Kh^2}{(h+K)^3D} - Gh^2\cos\theta\right]\end{array}\right]$$
$$+\frac{\bar{E}}{h+K} + \frac{k}{2\pi}Gh^2h_\eta\sin\theta + \left(\varepsilon\bar{E}\frac{5G}{24}\frac{k}{2\pi}h_\eta\left[\frac{3h^4+4h^3K}{(h+K)^2}\right]\sin\theta\right)$$
$$+\varepsilon\bar{E}P\left(\frac{h}{h+K}\right)^3\left[\frac{\bar{E}}{3(h+K)} + \frac{k}{2\pi}\frac{G}{120}(7h-15K)hh_\eta\sin\theta\right] = 0,$$

(10)

Equation (10) can also be written as a system of first order differential equations such that

The standard orthogonal collocation method is applied by evaluating the differential equations at N interior collocation points and setting this residual to zero The spatial discretization of (10) by the orthogonal collocation method at the collocation points results in a system of N ordinary differential equations over time.The discretization of the boundary conditions (2) gives us additional 4 equations. On the other hand we have only N+2 unknowns(h_i, $i=1,2.....,N+2$). Thus to get a consistent system of equations, we drop the equations at η_1,η_N such that we have N+2 equations in N+2 unknowns.

$$\frac{\partial h}{\partial \eta} = u_1 \qquad with \qquad h(0) = h_1$$

$$\frac{\partial u_1}{\partial \eta} = u_2 \qquad with \qquad u_1(1) = u_{1,N+1}$$

$$\frac{\partial u_2}{\partial \eta} = u_3 \qquad with \qquad u_2(0) = u_{2,1}$$

$$\frac{\partial u_3}{\partial \eta} = u_4 \qquad with \qquad u_3(1) = u_{3,N+1}$$

(11 a,b,c,d)

Equation (11.a) in terms of collocation matrices takes the form

$$\sum_{k=1}^{N+1} A'_{j+1,k} h_k = u_{1,j}, \qquad j = 1, 2, \ldots.., N$$

(12)

$\underset{\sim}{A'}$ is the weight matrix of first derivative for a boundary point at x=0.

Subroutines for the calculations of derivative weight matrices for orthogonal collocation up to second order are available in reference [6]. These are extended to any order in reference [7].

Equation (11b) can be written as follows

$$\sum_{j=1}^{N} A_{i-1,j} u_{1,j} + A_{i-1N+1} u_{1,N+1} = u_{2,i}, \qquad i = 2, 3\ldots.., N+1$$

(13)

$\underset{\sim}{A}$ is the matrix of first derivatives for the boundary point at x=1, and .

Substituting (12) into (13) leads to

$$\sum_{j=1}^{N} \sum_{k=1}^{N+1} A_{i-1,j} A'_{j+1,k} h_k + A_{i-1N+1} u_{1,N+1} = u_{2,i}, \qquad i = 2, 3\ldots.., N+1$$

(14)

But

$$A_{N+2-i,N+2-j} = -A'_{i,k}$$

$$\sum_{k=1}^{N+1} B_{i,k} h_k + A_{i-1N+1} u_{1,N+1} = u_{2,i}, \qquad i = 2, 3\ldots.., N$$

(15)

Where

$$B_{i,k} = -\sum_{j=1}^{N} A_{i-1,j} A_{N+1-j,N+2-k} \qquad \begin{array}{l} i = 2, \ldots, N+1 \\ k = 1, \ldots, N+1 \end{array}$$

(16)

The third first order differential equation (11c) can be written

$$A'_{i+1,1} u_{2,1} + \sum_{k=2}^{N+1} A'_{i+1,k} u_{2,k} = u_{3,i} \qquad i = 1, ..N$$

$$-A_{N+1-i,N+1} u_{2,1} - \sum_{k=2}^{N+1} \sum_{j=1}^{N+1} A_{N+1-i,N+2-k} B_{k,j} h_j - \sum_{k=2}^{N+1} A_{N+1-i,N+2-k} A_{k-1,N+1} u_{1,N+1} = u_{3,i}$$

(17)

the above equation can be expressed as

$$-A_{N+1-i,N+1} u_{2,1} + \sum_{j=1}^{N+1} BB_{i,j} h_j + B1_{i,N+1} u_{1,N+1} = u_{3,i}$$

(18)

where

$$BB_{i,j} = -\sum_{k=2}^{N+1} A_{N+1-i,N+2-k} B_{k,j}$$

$$B1_{i,N+1} = -\sum_{k=2}^{N+1} A_{N+1-i,N+2-k} A_{k-1,N+1} \qquad \begin{array}{l} i = 1, \ldots, N \\ j = 1, \ldots, N+1 \end{array}$$

(19)

the fourth ODE (equation 11d) is expressed

$$A_{i-1,N+1} u_{3,N+1} + \sum_{j=1}^{N} A_{i-1,j} u_{3,j} = u_{4,i} \qquad i = 2, ..N+1$$

$$-\sum_{j=1}^{N} A_{i-1,j} A_{N+1-j,N+1} u_{2,1} + \sum_{j=1}^{N} \sum_{k=1}^{N+1} A_{i-1,j} BB_{j,k} h_k + \sum_{j=1}^{N} A_{i-1,j} B1_{j,N+1} u_{1,N+1} = u_{4,i}$$

(20)

or

$$B2_{i,1}u_{2,1}+\sum_{k=1}^{N+1}BBB_{i,k}h_k+BB1_{i.N+1}u_{1,N+1}=u_{4,i}$$

(21)

where

$$B2_{i,1}=-\sum_{j=1}^{N}A_{i-1,j}A_{N+1-j,N+1}$$

$$BBB_{i,k}=\sum_{j=1}^{N}A_{i-1,j}BB_{j,k} \qquad \begin{matrix} i=2,\dots,N+1 \\ k=1,\dots,N+1 \end{matrix}$$

$$BB1_{i,N+1}=\sum_{j=1}^{N}A_{i-1,j}B1_{j,N+1}$$

(22)

The film thickness equation becomes

$$\begin{aligned} h_t+\frac{k^2\varepsilon}{4\pi^2}&\left[\begin{array}{l} \dfrac{k^2\bar{S}}{4\pi^2}\left(h^3u_4+3h^2u_1u_3\right)+ \\ u_2\left(\dfrac{A}{h}+\dfrac{2G^2}{15}h^6\sin^2\theta+\dfrac{KM}{P}\left(\dfrac{h}{h+K}\right)^2+\dfrac{E^2}{D}\left(\dfrac{h}{h+K}\right)^3-\dfrac{1}{3}Gh^3\cos\theta\right)+ \\ u_1^2\left[\dfrac{-A}{h^2}+\dfrac{2}{3}G^2h^5\sin^2\theta+\dfrac{2K^2Mh}{(h+K)^3P}+\dfrac{3Kh^2}{(h+K)^3D}-Gh^2\cos\theta\right] \end{array}\right] \\ &+\frac{\bar{E}}{h+K}+\frac{k}{2\pi}Gh^2u_1\sin\theta+\left(\varepsilon\bar{E}\frac{5G}{24}\frac{k}{2\pi}u_1\left[\frac{3h^4+4h^3K}{(h+K)^2}\right]\sin\theta\right) \\ &+\varepsilon\bar{E}P\left(\frac{h}{h+K}\right)^3\left[\frac{\bar{E}}{3(h+K)}+\frac{k}{2\pi}\frac{G}{120}(7h-15K)hu_1\sin\theta\right]=0, \end{aligned}$$

(23)

For the new formulation the boundary conditions are defined as follows

$$h(1)-h(0)=\int_0^1\frac{du_1}{d\eta}d\eta=0$$
$$=\sum_{j=1}^{N}w_j\frac{du_{1,j}}{d\eta}$$

(24.a)

$$u_1(1)-u_1(0)=\int_0^1\frac{du_2}{d\eta}d\eta=0$$
$$=\sum_{j=1}^{N}w_j\frac{du_{2,j+1}}{d\eta}=0$$

(24.b)

$$u_2(1)-u_2(0)=\int_0^1\frac{du_3}{d\eta}d\eta=0$$
$$=\sum_{j=1}^{N}w_j\frac{du_{3,j}}{d\eta}=0$$

(24.c)

$$u_3(1)-u_3(0)=\int_0^1\frac{du_4}{d\eta}d\eta=0$$
$$=\sum_{j=1}^{N}w_j\frac{du_{4,j+1}}{d\eta}=0$$

(24.d)

where w_j are the weights of the quadrature. We have N+4 equations in N+4 unknowns; N equations from the satisfaction of the differential equations at N collocation points, and four boundary conditions equations. We have N unknowns in h at N collocation points and 4 boundary points unknown, *h(0)*, $u_1(1)$, $u_2(0)$, $u_3(1)$.

Due to the steepness of the profile close to the rupture points in case of the presence of van der Waal forces, we may resort to the use of spline collocation method. In this case we divide the $\eta \in [0,1]$ into m splines. We will redefine η to $\bar{\eta}$ such that $\bar{\eta} = \frac{\eta}{m}$. In the governing equations we will replace $k/2\pi$ by $k/(2\pi m)$ and we will add in each spline, the following equations

$$h(k) - h(k-1) - \sum_{j=1}^{N} w_j \frac{du_{i,j+k(N-1)}}{d\eta'} = 0; \qquad k = 1,2,....,m \tag{25.a}$$

notice that h(m)=h(0)

$$u_1(k) - u_1(k-1) - \sum_{j=1}^{N} w_j \frac{du_{2,j+k(N-1)}}{d\eta'} = 0; \qquad k = 1,2,....,m \tag{25.b}$$

and $u_1(m)=u_1(0)$

$$u_2(k) - u_2(k-1) - \sum_{j=1}^{N} w_j \frac{du_{3,j+k(N-1)}}{d\eta'} = 0; \qquad k = 1,2,....,m \tag{25.c}$$

and $u_2(m)=u_2(0)$

$$u_3(k) - u_3(k-1) - \sum_{j=1}^{N} w_j \frac{du_{4,j+k(N-1)}}{d\eta'} = 0; \qquad k = 1,2,....,m \tag{25.d}$$

and $u_3(m)=u_3(0)$

The number of equations to solve are $n \times m$ governing equations plus $(m+1)\times 4$ boundary conditions. The number of unknowns is $(n+4)\times m+4$ which is equal to the number of equations and the boundary conditions. As we have shown above that the collocation method converts the evolution partial differential equation into a set of ordinary differential and algebraic equation. For the resulted system, a DAE (differential-algebraic-solver) is needed. We have chosen the DASSL FORTAN code to solve the system which is coded in FORTRAN. It uses backward differentiation formula methods to solve a system of DAE.

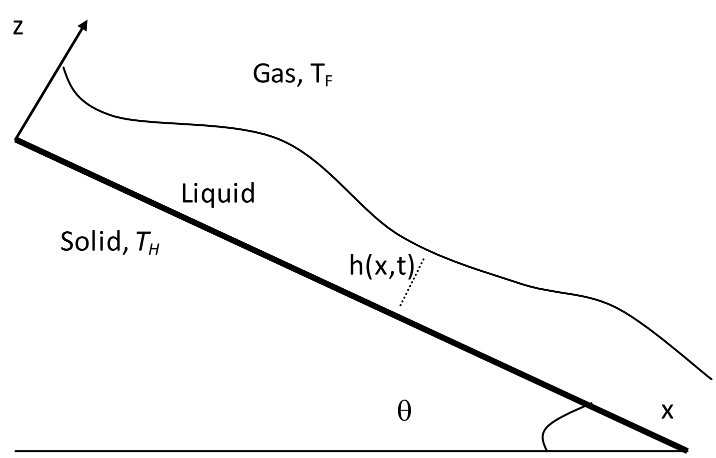

Fig. 1. Sketch of the inclined nonisothermal falling film.

Another solution scheme is derived to solve Eq.10 based on recasting the model into two second-order differential equations. The second derivative of the thickness is defined as

$$\frac{\partial^2 h}{\partial \eta^2} = v \tag{26}$$

This equation is written in term of the second-order derivative collocation matrix as

$$\sum_{j=1}^{N+2} B_{ij} h_j = v \tag{27}$$

the fourth-order derivative of the h can be defined as

$$\frac{\partial^4 h}{\partial \eta^4} = \frac{\partial^2 v}{\partial \eta^2} = \sum_{j=1}^{N+2}\sum_{k=1}^{N+1} B_{ik}B_{kj}h_j + B_{i,1}v_1 + B_{i,N+2}v_{N+2}$$

or

$$\frac{\partial^4 h}{\partial \eta^4} = \frac{\partial^2 v}{\partial \eta^2} = \sum_{j=1}^{N+2} BB_{ij}h_j + B_{i,1}v_1 + B_{i,N+2}v_{N+2} \tag{28}$$

where

$$BB_{ij} = \sum_{k=1}^{N+1} B_{ik}B_{kj}$$

The third-order derivative of h takes the form

$$\frac{\partial^3 h}{\partial \eta^3} = \frac{\partial\ v}{\partial \eta} = \sum_{j=1}^{N+2}\sum_{k=2}^{N+1} A_{ik}B_{kj}h_j + A_{i,1}v_1 + A_{i,N+2}v_{N+2}$$
$$= \sum_{j=1}^{N+2} AB_{ij}h_j + A_{i,1}v_1 + A_{i,N+2}v_{N+2}$$

where

$$AB_{ij} = \sum_{k=2}^{N+1} A_{ik}B_{kj}, \qquad i = 1,2,\ldots,N+2 \tag{29}$$

Thus we need to solve N differential equations at N collocation points

subject to four boundary conditions

$$h_1 = h_{N+2} \tag{30.a}$$

$$\sum_{j=1}^{N+2} A_{1,j}h_j = \sum_{j=1}^{N+2} A_{N+2,j}h_j \tag{30.b}$$

$$v_1 = v_{N+2} \tag{30.c}$$

$$A_{1,1}v_1 + A_{1,N+2}v_{N+2} + \sum_{j=1}^{N+2} A_{1,j}h_j = A_{1,1}v_1 + A_{1,N+2}v_{N+2} + \sum_{j=1}^{N+2} A_{N+2,j}h_j \tag{30.d}$$

So we have N+4 equation in N+4 unknowns (h_i, $i=1,2\ldots..,N+2$, v_1, v_{N+2})

For the case of horizontal plane,we could also use the symmetry of the equations around η=0, and write the initial conditions in a symmetric form;

$$f(x) = 1 + \delta\cos(2\pi\eta / k) \tag{31}$$

And then substitute;

$$\varsigma = 4\eta^2 \tag{32}$$

To obtain;

$$h_\eta = 4\sqrt{\varsigma}h_\zeta \tag{33}$$

and

$$h_{\eta\eta} = 16\varsigma h_{\zeta\zeta} + 8h_\zeta \tag{34}$$

Now we apply collocation in the new domain $\varsigma \in [0,1]$, corresponding to half length while satisfying the differential equations at N interior points . At $\zeta = 1$, we have;

$$\frac{\partial h}{\partial \zeta} = \frac{\partial v}{\partial \zeta} = 0 \tag{35}$$

So we have N+2 equations in N+2 unknowns (h_i, $i=1,2\ldots..,N+1$, v_{N+1})

We also have symmetry around $\zeta = 1$, so we can use spline collocation at $\zeta = \lambda$, such that we have continuity of the function and its first, second and third derivative at the spline point $\zeta = \lambda$, and apply the above second order approach on both sides of the spline point.

IV. RESULTS AND DISCUSSION

The input disturbance considered in the first part of this work is given as:

$$f(x) = 1 - 0.01\sin(2\pi\eta) \qquad \eta \in [0,1] \tag{36}$$

In the following we show and compare the results of three numerical methods;

1. The standard collocation (we call this S4).
2. Expanding the system equation to a set of first-order ODEs (N1)
3. Expanding the system equation to a set of first-order ODEs and using splines, we call this NS1
4. Expanding the system to a set of second-order differential equations, we call this N2.
5. Expanding the system to a set of second-order differential equations, and exploiting the symmetry around one point, we call this NS2
6. Expanding the system to a set of second-order differential equations, and exploiting the symmetry around two points, we call this NSS2

First we will study in details the following equation;

$$\frac{\partial h}{\partial t} + \frac{1}{8\pi^2}\left[\frac{1}{8\pi^2}\left(h^3\frac{\partial^4 h}{\partial \eta^4} + 3h^2\frac{\partial h}{\partial \eta}\frac{\partial^3 h}{\partial \eta^3}\right) - \frac{1}{h^2}\left(\frac{\partial h}{\partial \eta}\right)^2 + \frac{1}{h}\frac{\partial^2 h}{\partial \eta^2}\right] = 0, \tag{37}$$

Fig. 2 shows the film thickness dynamics simulated using the N1 method with 12 collocation points at the zeros of Legendre polynomials (Jacobi polynomials with α=β=0). It can be seen that the profile starts to oscillate as we approach rupture time. This is because as we approach rupture time the van der Waals forces of attraction becomes dominant and this leads to sharp gradient in the film height profile. Fig. 3 shows that 16 collocation points are needed to give accurate profile and rupture time. Fig. 4,5 shows that with 8 collocation points for S4 method the profile starts to deviate early in time. Fig. 6 shows that for t=9, N1 outperforms S4.

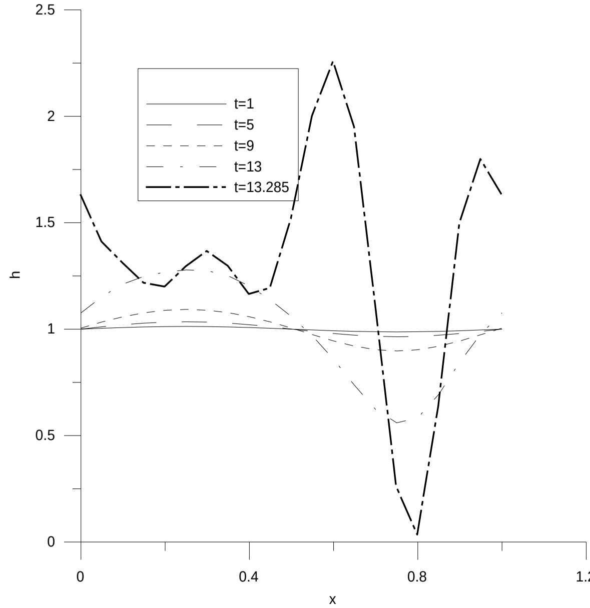

Fig. 2. Dynamic behavior of the film thickness with N=12 using N1.

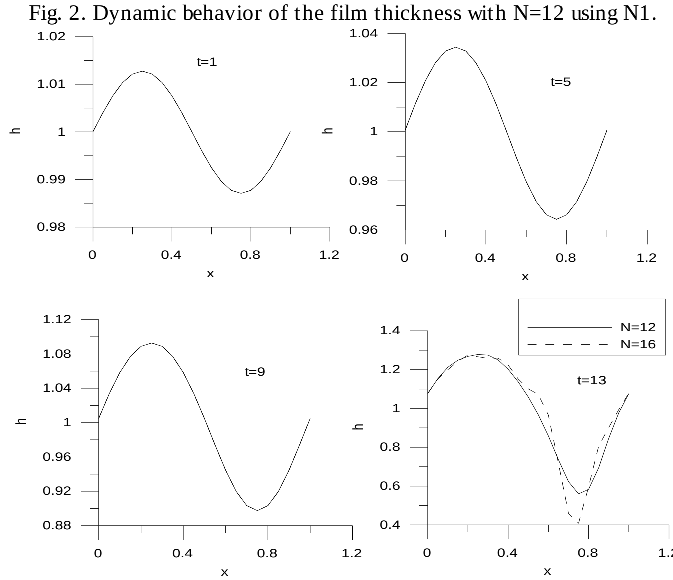

Fig. 3. Effect of increasing the collocation points for N1 at different times

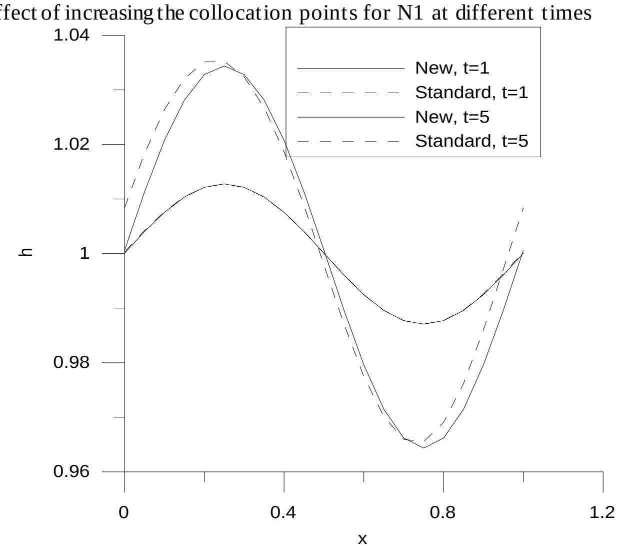

Fig. 4. Comparison of N1 (N=12) with S4 (N=8) at t=1,5.

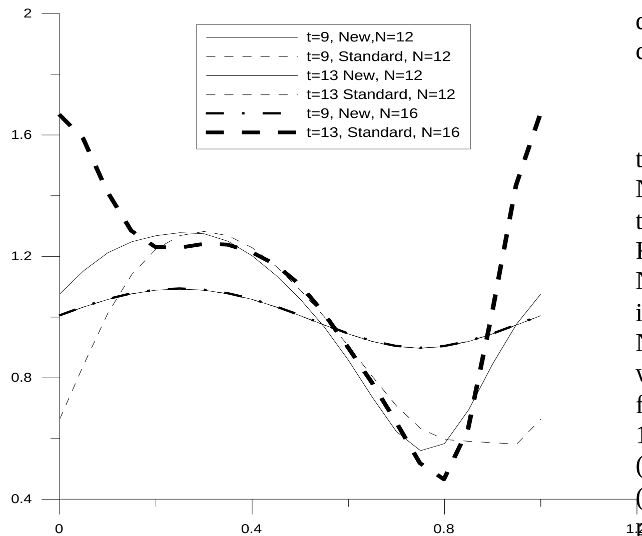

Fig. 5. Comparison of the new method (N1) with the standard method (S4).

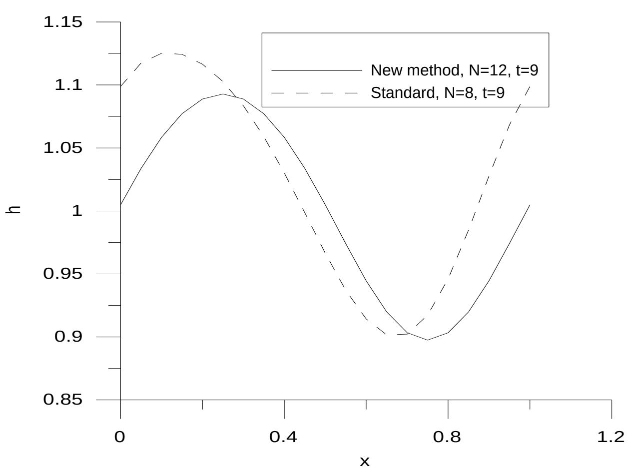

Fig. 6. Comparison of the new method(N1) with the standard method(S4) at t=9.

Fig. 7 shows that N2 gives oscillatory profile close to rupture time. Fig. 8 shows that at t=9, N2 gives satisfactory results for N=12, N=16. Fig. 9 shows the profiles for N2 at collocation points N=12, 16. It seems that there are some numerical inaccuracies occurring as we increase the time. Fig. 10 shows that N2 near rupture time gives unsatisfactory oscillating profile.

Rupture times are predicted using all three methods. We found that the first method N1 predicts the rupture time to be 13.285 with12 collocation points and 13.0 with 16 points. For the standard method prediction with 8 collocation points a rupture time of 13.27 is obtained. For N2 and N=16, a rupture time of about 13.02 is predicted. Based on these results we will exclude the standard method from further study. We would like to find a way to get accurate predictions for the rupture time since the evolution equation becomes singular at that time. First we thought if we could move the singularity to the boundary because the collocation method does not satisfy the differential equations at the boundary. This can be done if we change the inlet disturbance to

$$f(x) = 1 - 0.01\cos(2\pi\eta) \qquad \eta \in [0,1] \tag{38}$$

this leads to a shift in distance (x) by 0.75. For this case the N1 method is tested with 16 collocation points, the rupture time is found to be 13.157. The profile for t=13 is shown in Fig..11 and for t=13.157 it is shown in Fig. 12.

Next we used splines instead of global polynomials. So shown in Fig. 11, the height profiles for spline collocation method NS1 at t=13, and for (M=2,N=16),(M=2, N=8),and(M=4,N=4) where M indicates number of splines and where we used the first order derivative approach. They give similar profiles. Fig. 12 gives profiles close to rupture time for the cases (M=2,N=16),(M=1,N=16) and (M=2,N=8).The case of (M=2,N=16) gives the best results. Fig. 13 gives similar profiles for the cases of (M=1,N=16),(M=4,N=4),and (M=4,N=8). The case of (M=4,N=8) gives the best result and as good as (M=2, N=16) of Fig. 12. The second derivative spline method NS2 predicts the rupture time to be 13.158 with two splines and 8 collocation points in each spline. While the first-derivative spline method predicts the rupture time to be 13.157 with 4 splines and 8 collocation points. Similar results were obtained with 2 splines and 16 collocation points.

We conclude that the first order derivative approach gives the best results.

Burelbach et al [1] presented numerical results for the case when the amplitude of the initial condition forcing function is 0.1 instead of 0.01 used in this study. They used a finite difference method with 40 equal divisions for the solution of the governing equations. They gave a rupture time of 4.16394.The methods presented here gives a rupture time of 4.0835, e. g., M=4, N=8.

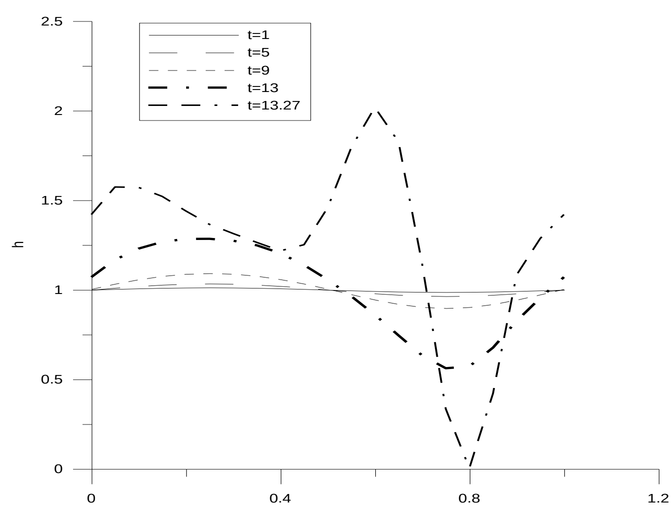

Fig. 7. Film thickness dynamics using the second-derivative approach N2.

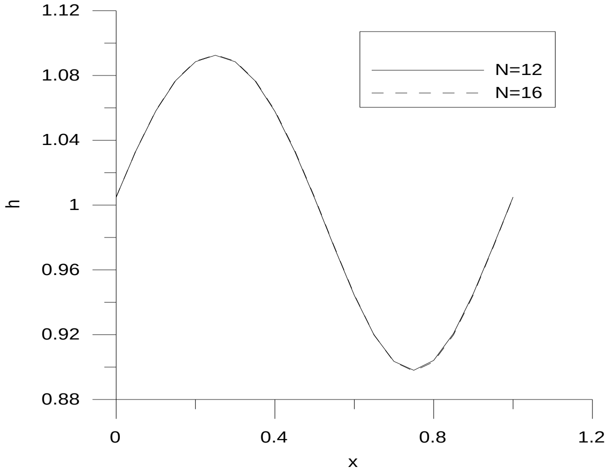

Fig. 8. Effects of the number of Collocation points on the film dynamics at t=9 for N2.

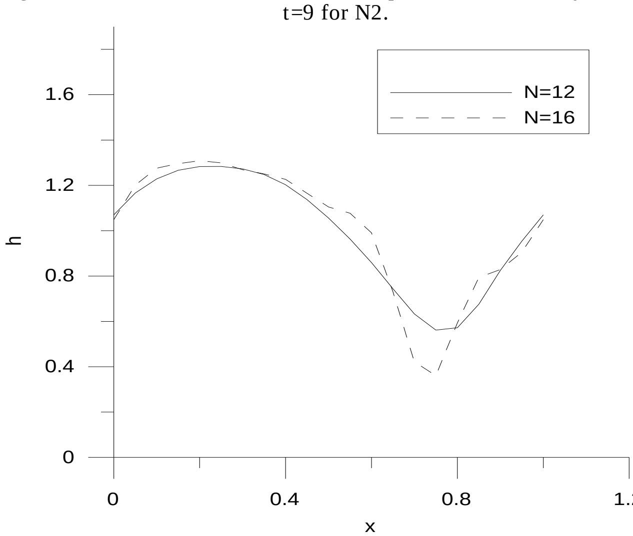

Fig. 9. Effects of the number of Collocation points on the film dynamics at t=13 for N2.

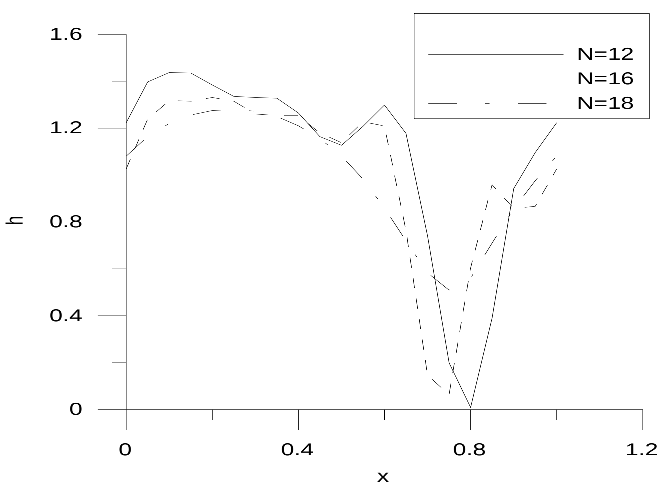

Fig. 10. Effects of the number of Collocation points on the film dynamics near the rupture time for N2.

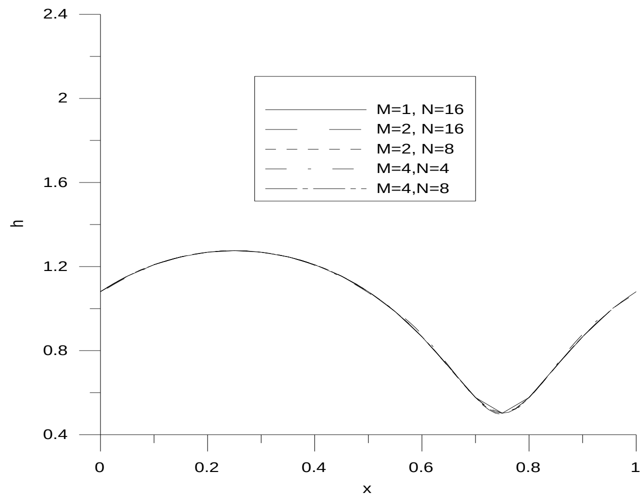

Fig. 11. Spline method prediction at t=13.

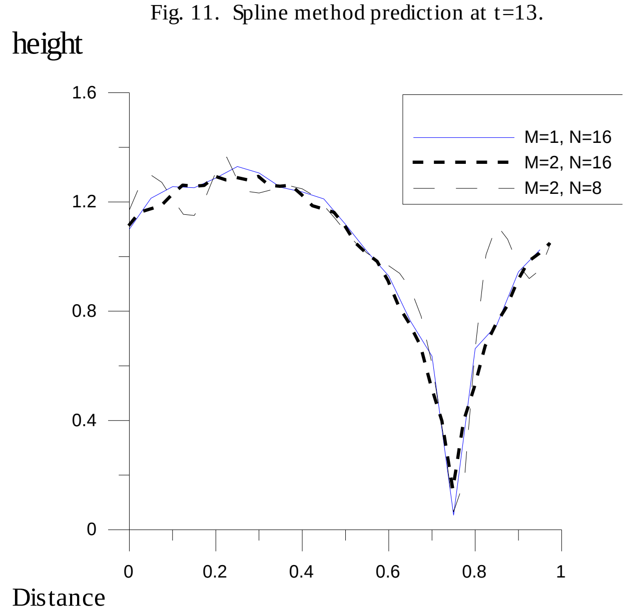

Fig. 12. 1-spline and 2-spline prediction close to the rupture time.

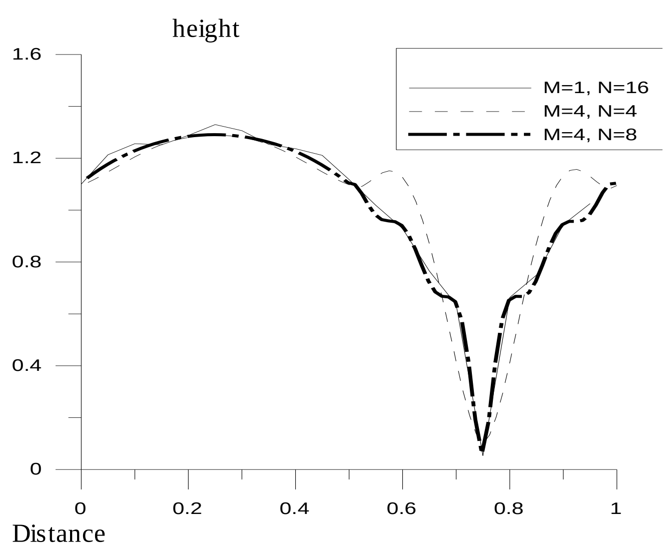

Fig. 13. 1-spline and 4-spline prediction close to the rupture time

IJENS

Now we test the NS2 and NSS2 schemes. A suitable choice for the weighting function of Jacobi polynomials in this case is [6,7],α=1,β=-0.5.The results are plotted in Fig. 14. For NS2 , we used N=18, and for NSS2 we used 8 points in each spline with λ=0.93. The same result is obtained for NSS2 if we use 12 points. The rupture time in all cases is 13.158. This is the most accurate solution. Thus both methods are recommended for horizontal symmetric problems. If we use NSS2 with 4 points at λ=0.87, we get the same rupture time but with some distortion in the profile.

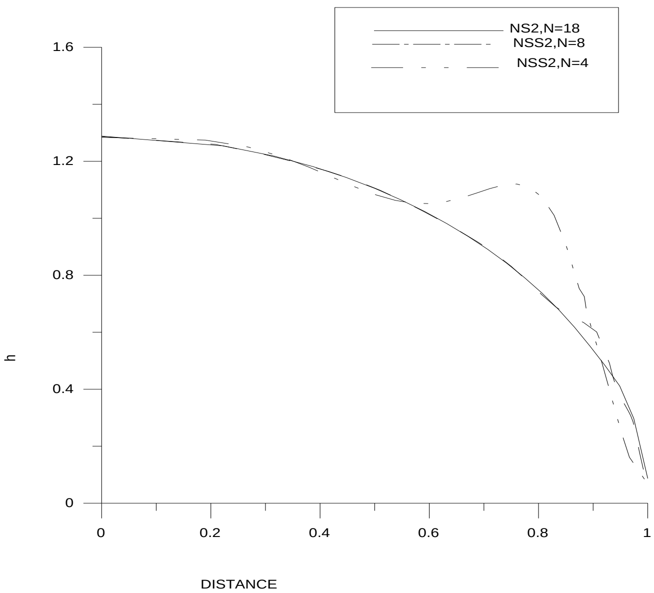

Fig. 14. Film thickness dynamics using the second-derivative approach NS2 & NSS2 near rupture time.

In the rest of this section we study the full equation (10), and uses the method NS1 with N=4 & M=16.We used the forcing function given by equation (31) with δ=0.1.

Data for the cases run are shown in Table I with the resulting rupture time shown in the last column. Fig. 15.a shows the thickness of an evaporating film at different times without van der Waal forces (A=0) and for k=0.5 when the vapor recoil is present

(E^2/D=2). Fig. 15.b shows the results for the same case but with the presence of weak van der Waal forces (A=0.01). The rupture time decreases when introducing the molecular forces. It can be seen that the profile near the trough becomes steeper as we approach the rupture time while at shorter times, the profiles for both cases are indistinguishable. Fig. 15.c shows the case of stronger van der Waal effect (A=0.1). A large A means that initial film thickness is very small and of nano-scale. The rupture time is shorter and the profile is steeper near the trough.

Fig.s 16.a.b.c. show the effect of increasing k on the film thickness for the cases A=0, 0.01 and 0.1 respectively. The local thinning near the trough becomes rapid enough to let the liquid flow producing two points rupture away from the middle point. It seems that increasing the van der Waal forces has only the effect of reducing rupture time but the profiles at rupture time are very similar.

Fig.s 17.a.b.c shows the case of no vapor recoil (E^2/D=0) but with large thermocapillarity (KM/P=2.0) and k=0.5. This introduces instability into the thickness profile. The new feature here is that as the trough gets closer to the plate surface, the film thickness profile becomes sharp and at earlier time, the profile is rather flat. The effect of van der Waal is to reduce the rupture time.

Fig.s 18.a.b.c show a similar case to Fig. 17.a.b.c but with larger k (k=1.0). Two points rapture occurs away from midpoint and this happens at shorter time.

Now in Fig.s 19a,b,c we study the effect of gravity on the behavior of evaporating film with no vapor recoil, thermocapillarity, van der Waal and k=0.7. Fig. 19.a shows the case of G=0 and Fig. 19.b is obtained with G=5.0. The gravity has a stabilizing effect and it increases the rupture time. Fig. 19.c represents the case of an inclined plane (q=45, G=5). Not only does the inclination reduce the rupture time but it increases also asymmetric wave with the location of rupture point shifted downstream.

Fig.s20.a.b.c presents the case of an inclined plane but with increasing van der Waal forces (A=0, 0.01, 0.1 respectively) and k=0.7. the main effect of van der Waal forcs is to reduce the rupture time.

Fig.s 21.a.b.c present the case of an inclined plane with increasing van der Waal forces (A=0, 0.01, 0.1 respectively) but with k=2.1. Now the rupture time is shifted upstream and again the rupture time decreases with increasing A.

TABLE I
PARAMETERS FOR THE SIMULATION RUNS.

Case	G,β	$\bar{S}$	$\bar{E}$	K	E^2/D	KM/P	A	P	k	ε	Rupture time
1	0,0	0.1	0.1	0.1	2.0	0	0	1	0.5	0.2	4.591
2	0,0	0.1	0.1	0.1	2.0	0	0.01	1	0.5	0.2	4.48
3	0,0	0.1	0.1	0.1	2.0	0	0.1	1	0.5	0.2	3.905
4	0,0	0.1	0.1	0.1	2.0	0	0.0	1	1.0	0.2	3.381
5	0,0	0.1	0.1	0.1	2.0	0	0.01	1	1.0	0.2	3.32
6	0,0	0.1	0.1	0.1	2.0	0	0.1	1	1.0	0.2	2.9
7	0,0	0.1	0.1	0.1	0	2	0.0	1	0.5	0.2	3.941
8	0,0	0.1	0.1	0.1	0	2	0.01	1	0.5	0.2	3.901
9	0,0	0.1	0.1	0.1	0	2	0.1	1	0.5	0.2	3.551
10	0,0	0.1	0.1	0.1	0	2	0.0	1	1.0	0.2	2.841
11	0,0	0.1	0.1	0.1	0	2	0.01	1	1.0	0.2	2.811
12	0,0	0.1	0.1	0.1	0	2	0.1	1	1.0	0.2	2,571
13	0,0	0.1	0.1	0.1	0	0	0	1	0.7	0.2	4.931
14	5,0	0.1	0.1	0.1	0	0	0	1	0.7	0.2	5.160
15	5, π/4	0.1	0.1	0.1	0	0	0.0	1	0.7	0.2	4.981
16	5, π/4	0.1	0.1	0.1	0	0	0.01	1	0.7	0.2	4.971
17	5, π/4	0.1	0.1	0.1	0	0	0.1	1	0.7	0.2	4.851
18	5, π/4	0.1	0.1	0.1	0	0	0.0	1	2.1	0.2	5.81
19	5, π/4	0.1	0.1	0.1	0	0	0.01	1	2.1	0.2	5.571
20	5, π/4	0.1	0.1	0.1	0	0	0.1	1	2.1	0.2	4.811

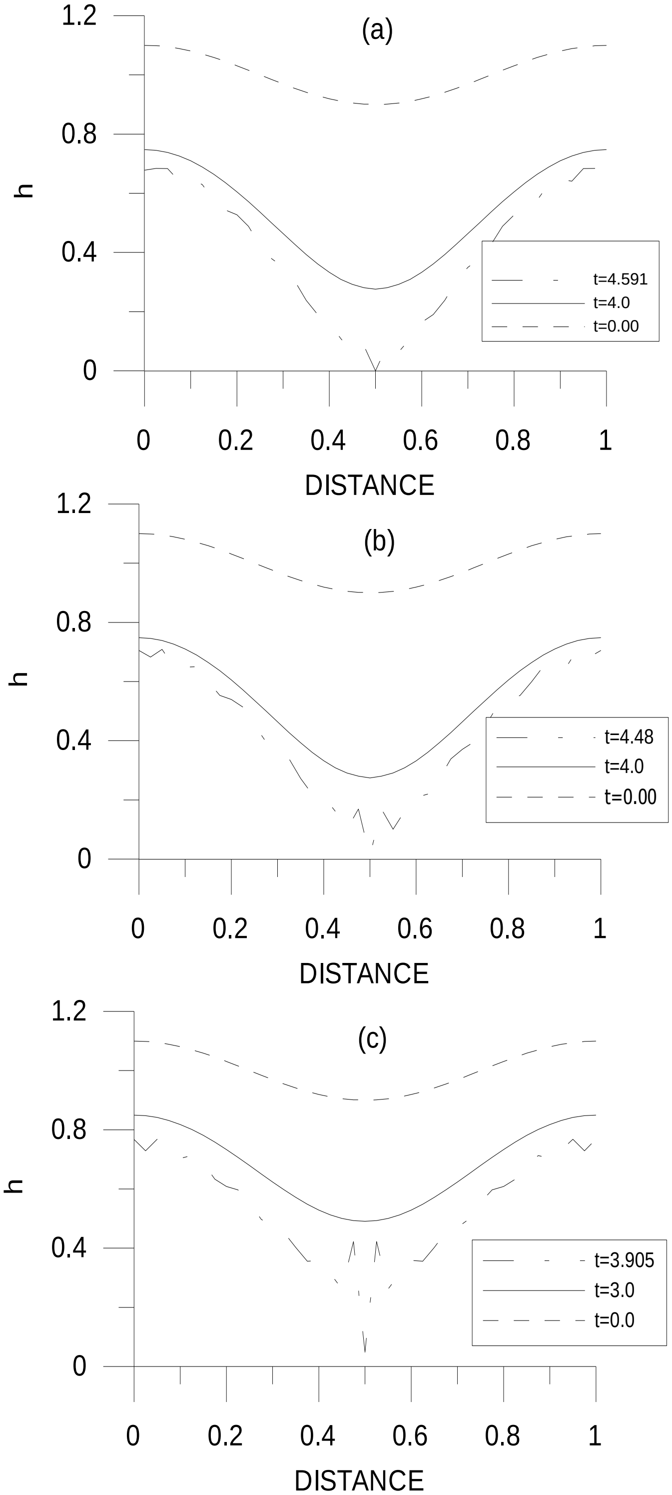

Fig. 15. Free surface evolution with vapour recoil and k=0.5. a)A=0, b) A=.01,c)A=.1

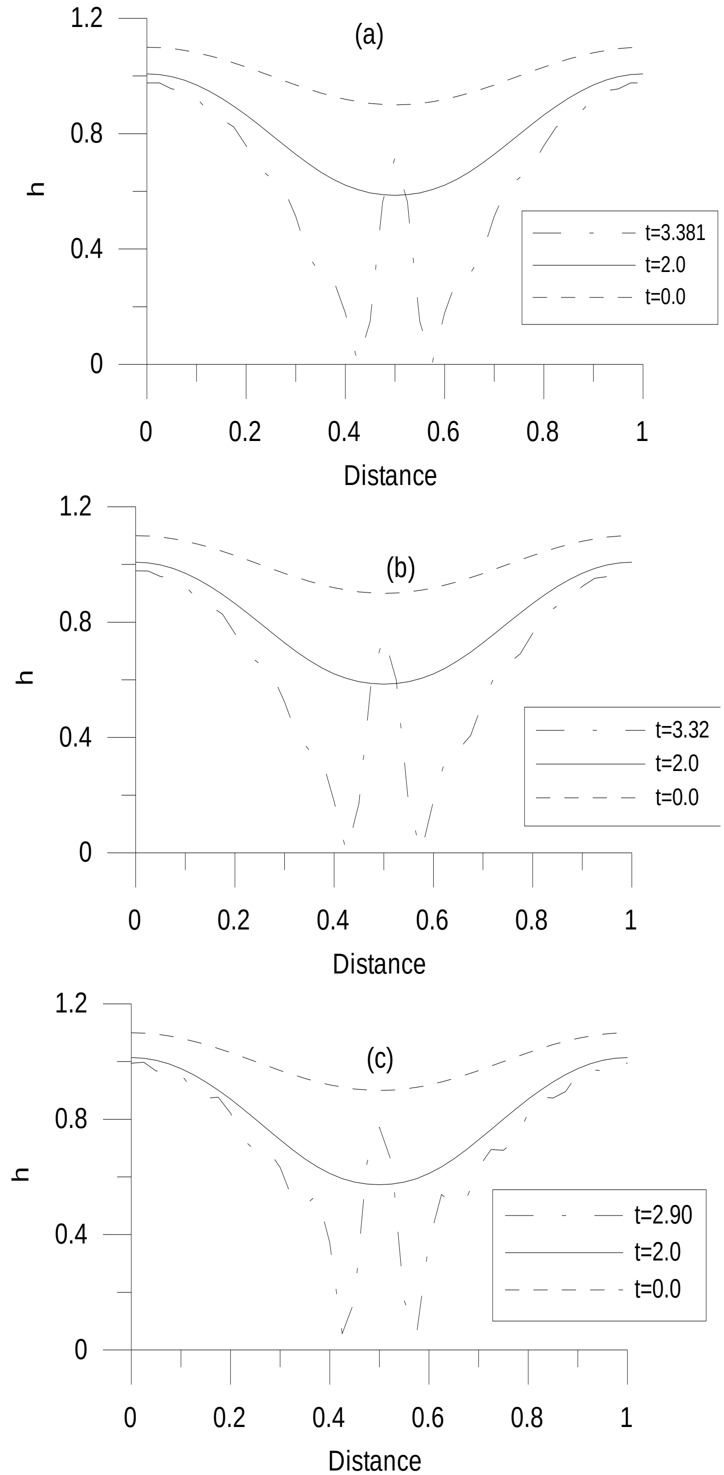

Fig. 16. Free surface evolution with vapour recoil and k=1, a)A=0, b) A=.01,c)A=.1

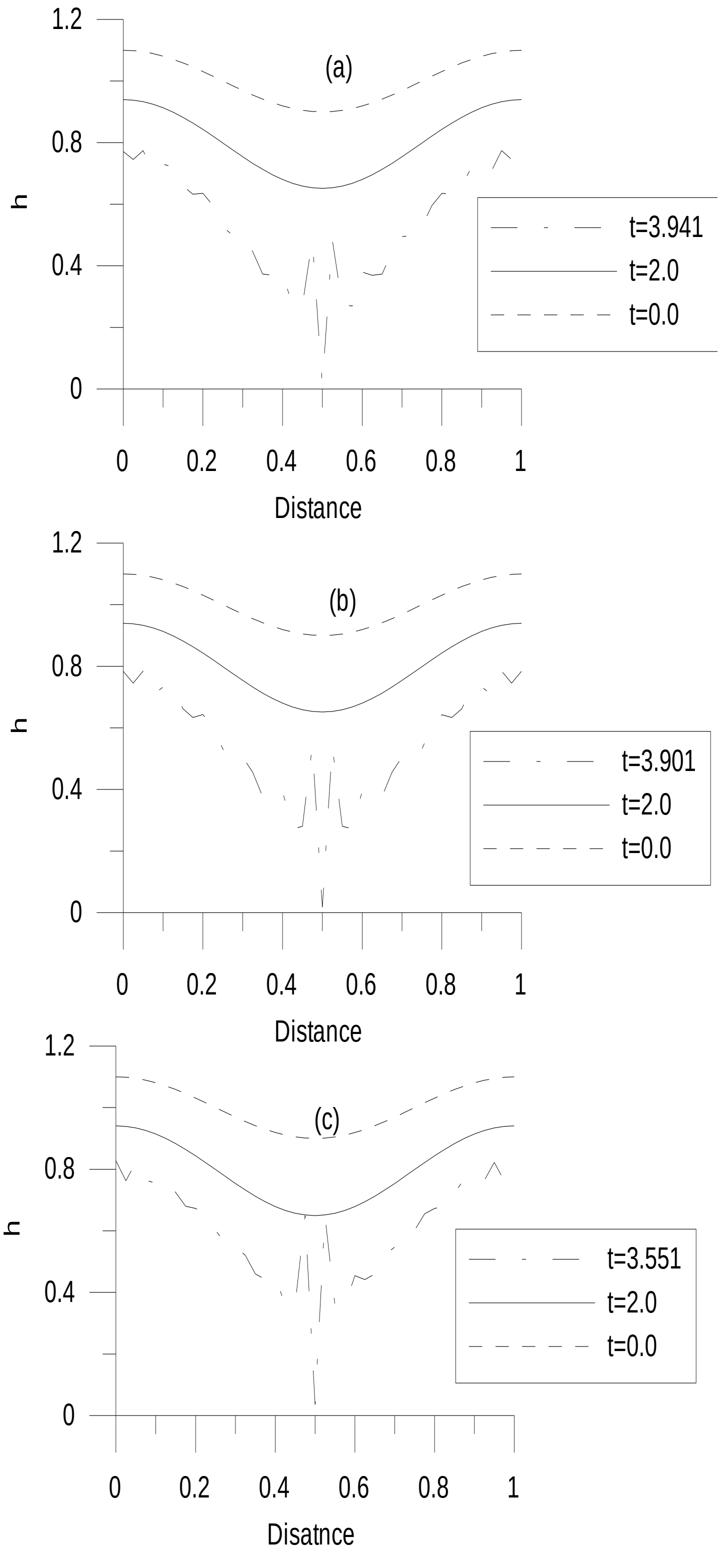

Fig. 17. Free surface evolution with thermocapillarity and k=.5, a)A=0, b) A=.01 c)A=.1

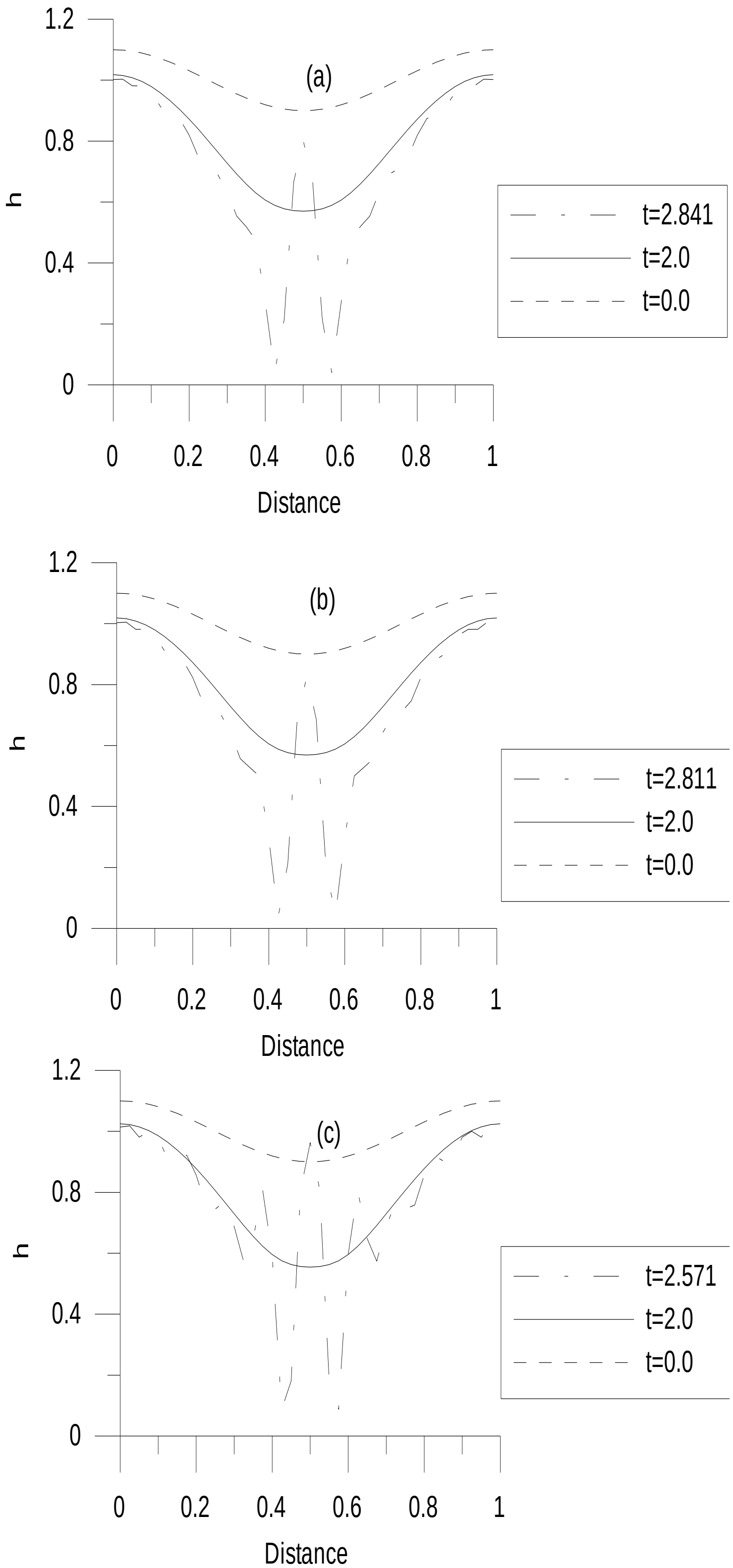

Fig. 18. Free surface evolution with thermocapillarity and k=1, a)A=0, b) A=.01 c)A=.1

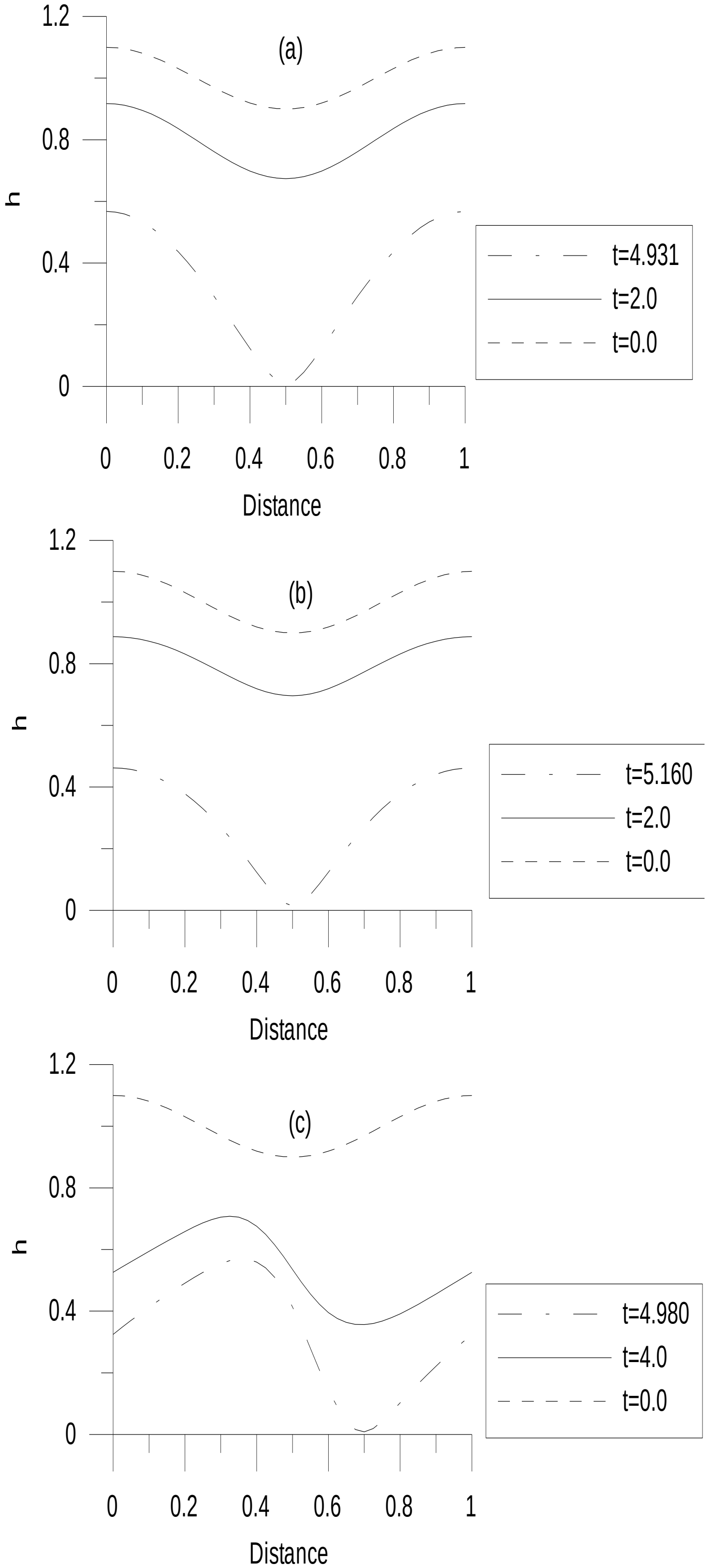

Fig. 19. Free surface evolution with gravity,k=.7,A=0,a)G=0,0,b)G=5,0,c)G=5,pi/4

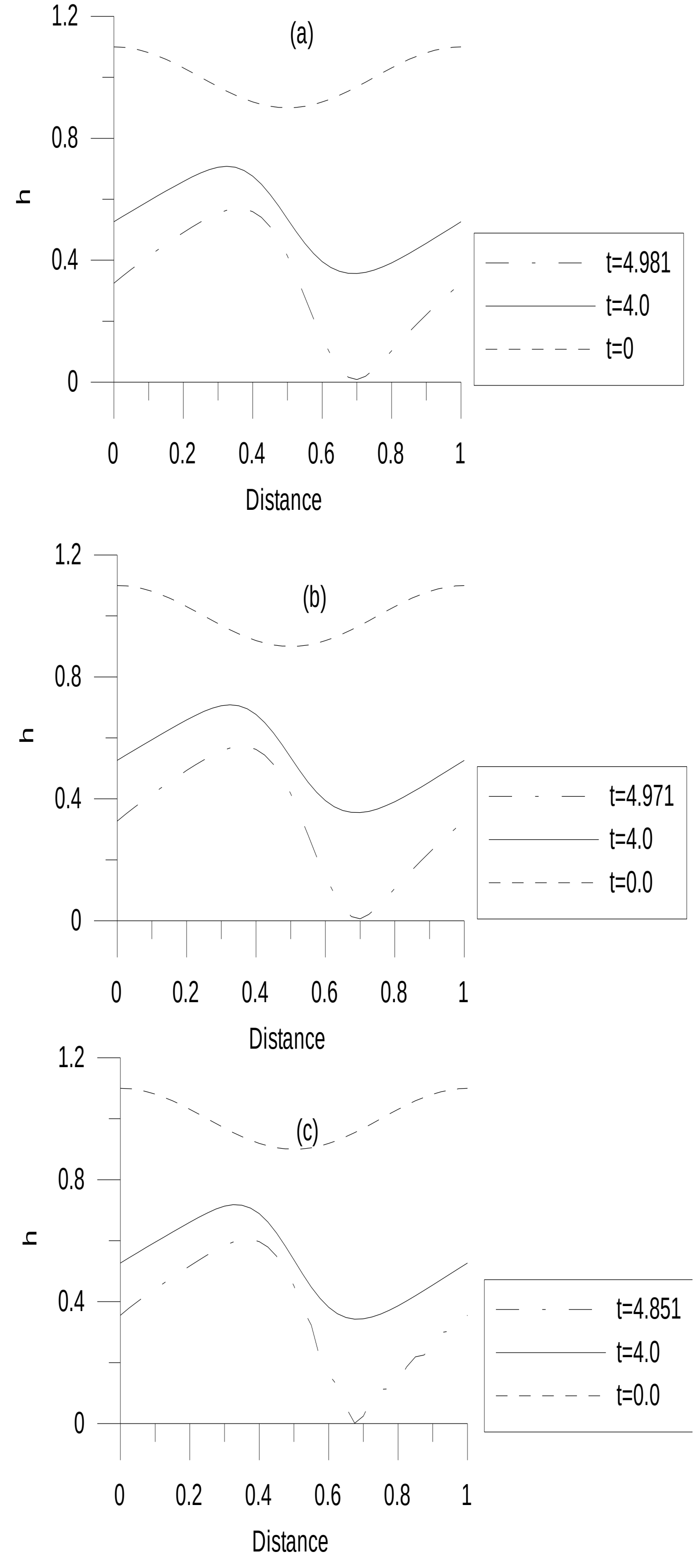

Fig. 20. Free surface evolution with gravity, G=5,pi/4,k=.7 a)A=0, b) A=.01,c)A=.1

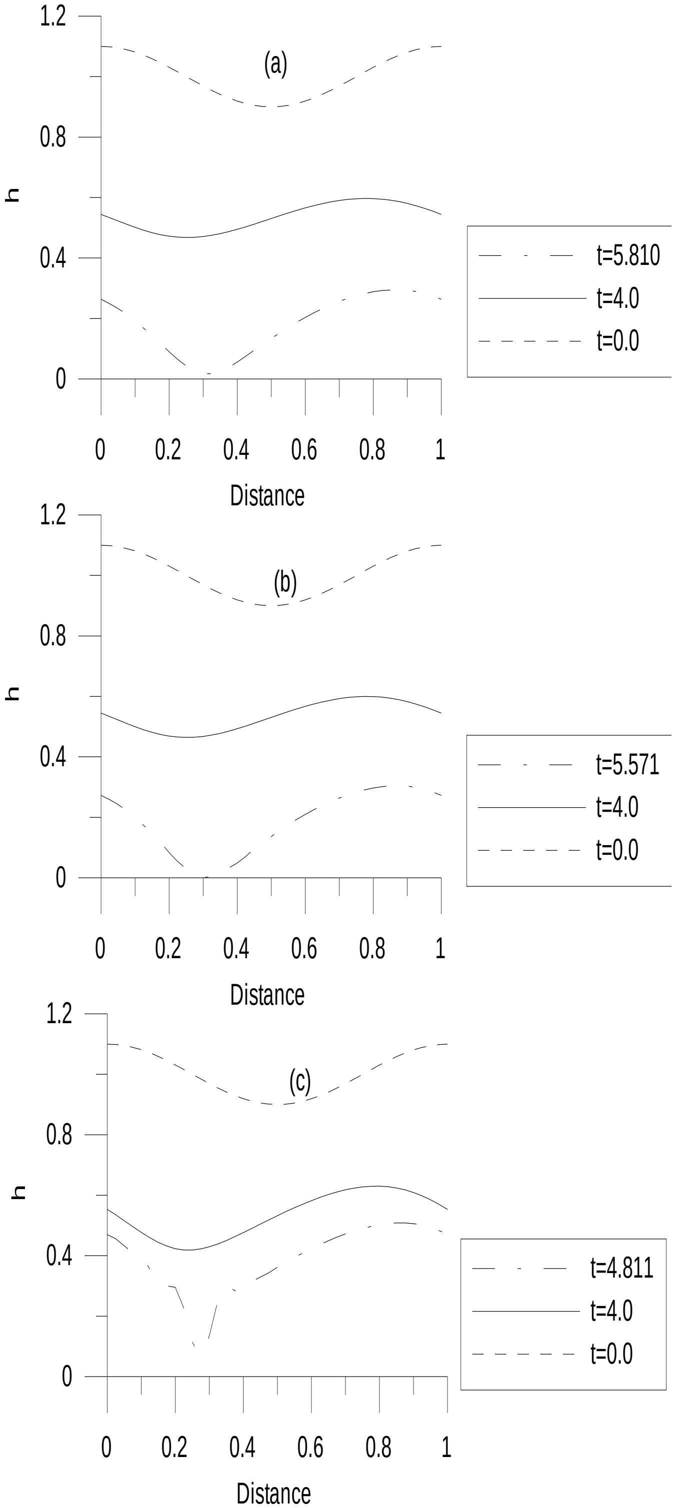

Fig. 21. Free surface evolution with gravity G=5,pi/4,k=2.1 a)A=0, b) A=.01,c)A=.1

CONCLUSIONS

The present work examines the dynamics of evaporating falling films of liquids on heated inclined planes taking into consideration intermolecular van der Waal forces which becomes active as the film gets thinner. As expected in all cases van der Waal forces reduce the rupture time of the falling films. Other factors which reduce rupture time include vapor recoil, thermocapillarity and increasing wave number and increasing the angle of inclination of the plane. Gravity, on the other hand, has a stability effect and increases rupture time. The numerical solution of the evolution equation is carried out using the collocation method. For symmetric cases where the plane is horizontal, a two spline collocation second order formulation method that makes use of the symmetry seems most appropriate. For inclined plane, a spline collocation first order formulation method is most efficient.

In summary, the numerical formulation presented here has direct applicability to other fourth order non-linear partial differential equations such as phase field model of infiltration[7]. Its usefulness should be tested in such applications. Comparison with other methods such as finite difference [1,6], and adaptive rational spectral methods needs also to be investigated.

REFERENCES

[1] Burelbach J. P. , Bankoff S. G. ,and Davis, S. H.,1988, Nonlinear Stability of Evaporating/ Condensing Liquid Films, J. Fluid Mech., 195,463-494

[2] Joo, S. W., Davis, S.W., and Bankoff, S.G., "Long wave Insatbilities of heated falling films", Journal of Fluid Mechanics, 230, pp.146-177 (1991).

[3] 3-Ali, M. A., Jameel A. T., and Ahmadun F. A., 2005, Stability and Rupture of Nano-Liquid Film (NLF) Flowing Down an Inclined Plane, Computers and Chemical Engineering, 29,2144-2154

[4] S. Miladinova , and G. Lebon, 2005, Effects of Nonuniform Heating and Thermocapillarity in Evaporating Films Falling down an Inclined Plane,Acta Mechanica, Vol 174, pp 33-49

[5] Reisfeld, B. and Bankoff S. G., 1992,"Non-isothermal flow of a liquid film on a horizontal cylinder ,J. Fluid Mech., 236:pp 167-196

[6] Momoniat, E. , Harley, C. , and Adlem, E.,2010, Numerical investigation of the generalized lubrication equation ,Applied Mathematics and Computation 217 , 2631–2638

[7] Cueto-Felgueroso, Luis, and Ruben Juanes,2009, "Adaptive rational spectral methods for the linear stability analysis of nonlinear fourth-order problems." Journal of Computational Physics 228.17: 6536-6552.

[8] Finlayson, B. (1980), Nonlinear Analysis in Chemical Engineering, McGraw-Hill, New York.

[9] Villadsen, J. and Michelsen M. J. (1978), Solution of Differential Equations Models by Polynomial Approximation, Prentice-Hall, New Jersey.

[10] Soliman, M. A. (2004),The Method of Orthogonal Collocation, King Saud University Press.